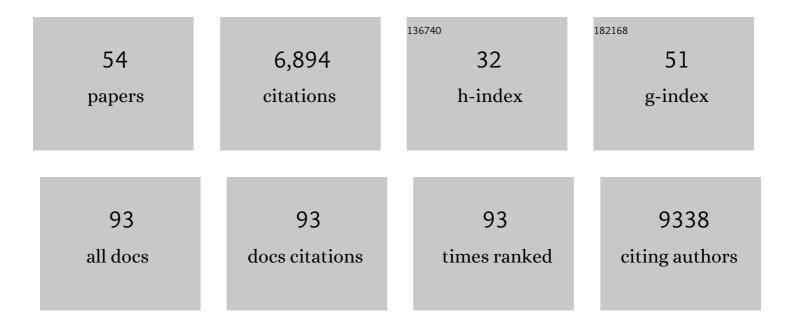
Adam Frost

List of Publications by Year in descending order

Source: https://exaly.com/author-pdf/8249361/publications.pdf Version: 2024-02-01



ADAM EDOST

| # | Article | IF | CITATIONS |
|----|--|------|-----------|
| 1 | Directed evolution of the rRNA methylating enzyme Cfr reveals molecular basis of antibiotic resistance. ELife, 2022, 11, . | 2.8 | 10 |
| 2 | A point mutation in the nucleotide exchange factor eIF2B constitutively activates the integrated stress response by allosteric modulation. ELife, 2022, 11, . | 2.8 | 5 |
| 3 | Primordial Protein Tails. Molecular Cell, 2021, 81, 6-7. | 4.5 | 2 |
| 4 | elF2B conformation and assembly state regulate the integrated stress response. ELife, 2021, 10, . | 2.8 | 46 |
| 5 | Photocatalytic LPOR forms helical lattices that shape membranes for chlorophyll synthesis. Nature Plants, 2021, 7, 437-444. | 4.7 | 35 |
| 6 | Activation of the Exocyst Tethering Complex for SNARE Complex Regulation and Membrane Fusion. FASEB Journal, 2021, 35, . | 0.2 | 0 |
| 7 | Ribosome-associated quality control and CAT tailing. Critical Reviews in Biochemistry and Molecular Biology, 2021, 56, 603-620. | 2.3 | 14 |
| 8 | Practical considerations for using K3 cameras in CDS mode for high-resolution and high-throughput single particle cryo-EM. Journal of Structural Biology, 2021, 213, 107745. | 1.3 | 33 |
| 9 | Viral evasion of the integrated stress response through antagonism of eIF2-P binding to eIF2B. Nature Communications, 2021, 12, 7103. | 5.8 | 14 |
| 10 | Comparative host-coronavirus protein interaction networks reveal pan-viral disease mechanisms. Science, 2020, 370, . | 6.0 | 508 |
| 11 | GIGYF2 and 4EHP Inhibit Translation Initiation of Defective Messenger RNAs to Assist Ribosome-Associated Quality Control. Molecular Cell, 2020, 79, 950-962.e6. | 4.5 | 119 |
| 12 | Anisotropic ESCRT-III architecture governs helical membrane tube formation. Nature Communications, 2020, 11, 1516. | 5.8 | 55 |
| 13 | Membrane Constriction and Thinning by Sequential ESCRT-III Polymerization. Biophysical Journal, 2020, 118, 88a. | 0.2 | 2 |
| 14 | Assessment of the nucleotide modifications in the high-resolution cryo-electron microscopy structure of the Escherichia coli 50S subunit. Nucleic Acids Research, 2020, 48, 2723-2732. | 6.5 | 22 |
| 15 | Exocyst structural changes associated with activation of tethering downstream of Rho/Cdc42 GTPases. Journal of Cell Biology, 2020, 219, . | 2.3 | 32 |
| 16 | LEM2 phase separation promotes ESCRT-mediated nuclear envelope reformation. Nature, 2020, 582, 115-118. | 13.7 | 97 |
| 17 | Membrane constriction and thinning by sequential ESCRT-III polymerization. Nature Structural and Molecular Biology, 2020, 27, 392-399. | 3.6 | 77 |
| 18 | Dynamin regulates the dynamics and mechanical strength of the actin cytoskeleton as a multifilament actin-bundling protein. Nature Cell Biology, 2020, 22, 674-688. | 4.6 | 70 |

Adam Frost

| # | Article | IF | CITATIONS |
|----|---|------|-----------|
| 19 | Structural and mechanistic basis of the EMC-dependent biogenesis of distinct transmembrane clients. ELife, 2020, 9, . | 2.8 | 66 |
| 20 | Open and cut: allosteric motion and membrane fission by dynamin superfamily proteins. Molecular Biology of the Cell, 2019, 30, 2097-2104. | 0.9 | 11 |
| 21 | Current outcomes when optimizing â€~standard' sample preparation for singleâ€particle cryoâ€EM. Journal of Microscopy, 2019, 276, 39-45. | 0.8 | 41 |
| 22 | Functional role of PGAM5 multimeric assemblies and their polymerization into filaments. Nature Communications, 2019, 10, 531. | 5.8 | 30 |
| 23 | A Tunable Microfluidic Device Enables Cargo Encapsulation by Cell―or Organelleâ€Sized Lipid Vesicles Comprising Asymmetric Lipid Bilayers. Advanced Biology, 2019, 3, 1900010. | 3.0 | 10 |
| 24 | elF2B-catalyzed nucleotide exchange and phosphoregulation by the integrated stress response. Science, 2019, 364, 491-495. | 6.0 | 96 |
| 25 | Structure of the nucleotide exchange factor eIF2B reveals mechanism of memory-enhancing molecule. Science, 2018, 359, . | 6.0 | 143 |
| 26 | The ER membrane protein complex interacts cotranslationally to enable biogenesis of multipass membrane proteins. ELife, 2018, 7, . | 2.8 | 160 |
| 27 | FDM 3D Printing of High-Pressure, Heat-Resistant, Transparent Microfluidic Devices. Analytical Chemistry, 2018, 90, 10450-10456. | 3.2 | 91 |
| 28 | Structures, Functions, and Dynamics of ESCRT-III/Vps4 Membrane Remodeling and Fission Complexes. Annual Review of Cell and Developmental Biology, 2018, 34, 85-109. | 4.0 | 205 |
| 29 | Vms1p is a release factor for the ribosome-associated quality control complex. Nature Communications, 2018, 9, 2197. | 5.8 | 80 |
| 30 | Structural basis of mitochondrial receptor binding and constriction by DRP1. Nature, 2018, 558, 401-405. | 13.7 | 219 |
| 31 | LEM2 recruits CHMP7 for ESCRT-mediated nuclear envelope closure in fission yeast and human cells. Proceedings of the National Academy of Sciences of the United States of America, 2017, 114, E2166-E2175. | 3.3 | 149 |
| 32 | CAT-tailing as a fail-safe mechanism for efficient degradation of stalled nascent polypeptides. Science, 2017, 357, 414-417. | 6.0 | 113 |
| 33 | Structural inhibition of dynamin-mediated membrane fission by endophilin. ELife, 2017, 6, . | 2.8 | 40 |
| 34 | In vitro analysis of RQC activities provides insights into the mechanism and function of CAT tailing. ELife, 2017, 6, . | 2.8 | 55 |
| 35 | Membrane fission by dynamin: what we know and what we need to know. EMBO Journal, 2016, 35, 2270-2284. | 3.5 | 388 |
| 36 | A Golgi rhomboid protease Rbd2 recruits Cdc48 to cleave yeast SREBP. EMBO Journal, 2016, 35, 2332-2349. | 3.5 | 36 |

Adam Frost

| # | Article | IF | CITATIONS |
|----|--|------|-----------|
| 37 | Double agents for mitochondrial division. Nature, 2016, 540, 43-44. | 13.7 | 7 |
| 38 | Subunit connectivity, assembly determinants and architecture of the yeast exocyst complex. Nature Structural and Molecular Biology, 2016, 23, 59-66. | 3.6 | 108 |
| 39 | Structural and functional studies of membrane remodeling machines. Methods in Cell Biology, 2015, 128, 165-200. | 0.5 | 7 |
| 40 | Structure and membrane remodeling activity of ESCRT-III helical polymers. Science, 2015, 350, 1548-1551. | 6.0 | 230 |
| 41 | Rqc2p and 60 <i>S</i> ribosomal subunits mediate mRNA-independent elongation of nascent chains. Science, 2015, 347, 75-78. | 6.0 | 245 |
| 42 | Molecular Mechanism of ESCRTâ€III Filament Formation. FASEB Journal, 2015, 29, 886.19. | 0.2 | 0 |
| 43 | Interchangeable adaptors regulate mitochondrial dynamin assembly for membrane scission. Proceedings of the National Academy of Sciences of the United States of America, 2013, 110, E1342-51. | 3.3 | 158 |
| 44 | Visualizing BAR-Dependent Membrane Remodeling. Microscopy and Microanalysis, 2012, 18, 44-45. | 0.2 | 0 |
| 45 | A Ribosome-Bound Quality Control Complex Triggers Degradation of Nascent Peptides and Signals Translation Stress. Cell, 2012, 151, 1042-1054. | 13.5 | 536 |
| 46 | Structural Basis of Membrane Bending by the N-BAR Protein Endophilin. Cell, 2012, 149, 137-145. | 13.5 | 220 |
| 47 | Functional Repurposing Revealed by Comparing S.Âpombe and S.Âcerevisiae Genetic Interactions. Cell, 2012, 149, 1339-1352. | 13.5 | 154 |
| 48 | Membrane Trafficking: Decoding Vesicle Identity with Contrasting Chemistries. Current Biology, 2011, 21, R811-R813. | 1.8 | 3 |
| 49 | The BAR Domain Superfamily: Membrane-Molding Macromolecules. Cell, 2009, 137, 191-196. | 13.5 | 522 |
| 50 | The F-BAR Domain of srGAP2 Induces Membrane Protrusions Required for Neuronal Migration and Morphogenesis. Cell, 2009, 138, 990-1004. | 13.5 | 306 |
| 51 | Structural Basis of Membrane Invagination by F-BAR Domains. Cell, 2008, 132, 807-817. | 13.5 | 509 |
| 52 | F-BAR Proteins Join the BAR Family Fold. Structure, 2007, 15, 751-753. | 1.6 | 49 |
| 53 | GTP-dependent twisting of dynamin implicates constriction and tension in membrane fission. Nature, 2006, 441, 528-531. | 13.7 | 432 |
| 54 | The Docking Protein FRS2α Controls a MAP Kinase-Mediated Negative Feedback Mechanism for Signaling by FGF Receptors. Molecular Cell, 2002, 10, 709-719. | 4.5 | 142 |